

12-2014

A Portable Impedance Biosensing System based on a Laptop with LabVIEW for Rapid Detection of Avian Influenza Virus

Yixiang Wang

University of Arkansas, Fayetteville

Follow this and additional works at: <http://scholarworks.uark.edu/etd>

 Part of the [Biomedical Devices and Instrumentation Commons](#), and the [Virology Commons](#)

Recommended Citation

Wang, Yixiang, "A Portable Impedance Biosensing System based on a Laptop with LabVIEW for Rapid Detection of Avian Influenza Virus" (2014). *Theses and Dissertations*. 2100.
<http://scholarworks.uark.edu/etd/2100>

This Thesis is brought to you for free and open access by ScholarWorks@UARK. It has been accepted for inclusion in Theses and Dissertations by an authorized administrator of ScholarWorks@UARK. For more information, please contact scholar@uark.edu, ccmiddle@uark.edu.

A Portable Impedance Biosensing System based on a Laptop with LabVIEW for Rapid
Detection of Avian Influenza Virus

A Portable Impedance Biosensing System based on a Laptop with LabVIEW for Rapid
Detection of Avian Influenza Virus

A thesis submitted in partial fulfillment
of the requirements for the degree of
Master of Science in Biological Engineering

by

Yixiang Wang
Shandong University of Science and Technology
Bachelor of Science in Electronic and Information Engineering, 2012

December 2014
University of Arkansas

This thesis is approved for recommendation to the Graduate Council.

Dr. Yanbin Li

Thesis Director

Dr. Thomas A. Costello

Committee Member

Dr. Michael F. Slavik

Committee Member

Abstract

Avian Influenza Virus (AIV) H5N1 is a highly pathogenic virus found not only in birds but also in human. Rapid and sensitive detection method is needed to help prevent the spread of AIV H5N1. In this study, a portable impedance biosensing system based on a laptop with LabVIEW software was developed for detection of AIV H5N1. First, a virtual instrument was programmed with LabVIEW software to form a platform for impedance measurement, data processing and control. The audio card of a laptop was used as a function generator while a data acquisition card was used with the signal channels for data communication. A gold interdigitated microelectrode was coated with specific aptamers to bind H5N1 virus and used in a microflow cell to obtain changes in impedance with desired accuracy and sensitivity. A sampling delivery unit consisted of a pump and three valves and was controlled by the virtual instrument to provide automated operation with adjustable flow rate. Results of the impedance measured with this biosensing system were compared with a commercial IM 6 impedance analyzer, and the error was less than 5%. The experiments on AIV H5N1 virus showed a linear relationship between the impedance change and the concentration of AIV H5N1 in a detection range from 2 to 16HAU. The specificity for detection of AIV H5N1 was confirmed with three non-target AIV subtypes, H1N1, H5N2, and H5N3. The biosensing system is portable and automated and has great potential to serve as a diagnostic and epidemiological tool for in-field rapid detection of AIV and other pathogens.

Keywords: Avian influenza virus H5N1, virtual instrument, impedance measurement, virus detection

Acknowledgements

First I would like to thank my major advisor, Dr. Yanbin Li, for his inspiring advice and continuous encouragement during my graduate education. He provided enough space for independent thinking while he pointed out the right direction when I was confused. He not only taught me how to think, but also how to learn. The passion for research from him encouraged me throughout my research. All of these lessons he has taught me will always stay in my mind and guide me in my future career.

I would also like to thank my advisory committee members, Dr. Thomas Costello and Dr. Michael Slavik. I do really appreciate their time and suggestions for this thesis.

I want to thank the researchers that offered help for this study: Dr. Tiemin Zhang of South China Agricultural University for fabricating the flow cell; Dr. Benhua Zhang of Shenyang Agricultural University for designing the virtual impedance analyzer; Dr. Huaguang Lu of Penn State University for providing non-target viruses.

Also I need to thank the research group for their support: Dr. Ronghui Wang for her advice and help on the research related things; Sardar Abdallah for his experience on preparing the microelectrodes; Zach Callaway for being a great friend, answering my endless questions and offering his help in the lab.

I would like to thank the Department of Biological Engineering for supporting me with a teaching assistantship and Center of Excellence for Poultry Science for providing the lab for tests.

Lastly, I would like to thank my parents and all my friends for always being a sun there kept warming me up when I was down. The love and support from them will be in the bottom of my heart, forever.

Table of Contents

Chapter 1 Introduction.....	1
Chapter 2 Objectives.....	4
Chapter 3 Review of Literature.....	6
3.1 Influenza A Virus.....	7
3.2 Current Methods of H5N1 Detection.....	9
3.3 Biosensors.....	11
3.3.1 Major Types of Biosensors Used in Microbial Detection.....	12
3.3.2 Impedance Measurement and Impedance Biosensors.....	13
3.3.3 Aptamers.....	15
3.4 Impedance Measurement and Impedance Biosensors.....	16
3.5 Microfluidics.....	16
3.6 LabVIEW Software	17
Chapter 4 Materials and Methods.....	19
4.1 Materials.....	20
4.1.1 Biological and Chemical Reagents.....	20
4.1.2 InterdigitatedArray Microelectrodes and Flow Cell.....	21

4.1.3 Micro-Pumps and Valves.....	22
4.1.4 Laptop and DAQ.....	23
4.2 Detection of AIV H5N1.....	23
4.2.1 Pretreatment of Microelectrodes.....	23
4.2.2 Impedance Measurement.....	23
4.3 Operation of the Biosensing System.....	25
Chapter 5 Results and Discussion.....	27
5.1 Design and Fabrication of the Biosensing System.....	28
5.1.1 Software Design and Fabrication.....	29
5.1.2 Hardware Design and Fabrication.....	30
5.2 Comparison of Impedance Measurements.....	32
5.3 Specificity for Detection of AIV H5N1.....	34
5.4 Impedance Responses to the Different Concentrations of AIV H5N1	36
Chapter 6 Conclusions.....	38
Chapter 7 Recommendations for Future Research.....	40
References.....	42

List of Tables

Table 5.1- Sequential control of the sample delivering system.....	30
Table 5.2 - Impedance measured by IM6 and the developed biosensor system. The frequency point chosen was 108 Hz.....	34
Table 5.3 - Impedance measured at 108 Hz recorded by the biosensing system for the target H5N1 virus along with the three non-target AIV subtypes at 8 HAU.....	35
Table 5.4 - Impedance measured at 108 Hz for different concentration of the target AIV H5N1 virus.....	37

List of Figures

Figure 3.1 - Elements of a biosensor.....	12
Figure 4.1 - Secondary structure of the H5N1 aptamer (Adopted from Wang and Li, 2013)	21
Figure 4.2 - (a) The front view of the flow cell and (b) the microchannels for sample delivery (diameter: 1mm, length: 8 mm) (Zhang and Li, 2013).....	22
Figure 4.3 - Gold interdigitated array microelectrode.	22
Figure 4.4 - (a) The SP 100 series pump and (b) 120 SP series valves connected to tubings.....	23
Figure 4.5 - The virtual impedance analyzer developed in LabVIEW (Adopted from Zhang et al., 2013).	24
Figure 4.6 - (a) The structure and components of the virtual impedance analyzer and (b) the circuit of measurement (Adopted from Zhang et al., 2013).....	24
Figure 4.7 - Block diagram design of the virtual impedance analyzer (Adopted from Zhang, 2013).....	25
Figure 5.1 - Structure of the biosensing system.	28
Figure 5.2 - (a) Front panel design and (b) block diagram of the virtual instrument for control.....	29
Figure 5.3 - (a) Circuit design of the sample delivery system and (b) the whole hardware system.....	31
Figure 5.4 - (a), (c) and (e) Impedance measured from three IDA microelectrodes by IM6 and (b), (d) and (f) developed biosensor system. The H5N1 sample concentration was 8 HAU.....	33

Figure 5.5 - Impedance changes at 108 Hz recorded by the biosensing system for the target H5N1 virus along with the three non-target AIV subtypes at 8 HAU. The means and error bars were calculated based on 2 replicates.....35

Figure 5.6 - Impedance changes at 108 Hz recorded by the biosensing system for different concentration of the target AIV H5N1 virus. The means and error bars were calculated based on 2 replicates.....37

Chapter 1 Introduction

Avian influenza H5N1 has caused significant health problem worldwide with the first case of highly pathogenic AIV H5N1 discovered in the late 1990s. A global H5N1 flu pandemic could kill 2-7.4 million people (CDC, 2010). 150 million poultry died from H5N1 infection and more than \$10 billion was lost due to H5N1 directly or indirectly in about ten years. More than 630 H5N1 human cases were found since 2003 with a mortality rate about 60% (WHO, 2012). Further investigation shows that the probable spread of H5N1 among human occurred in Thailand. Study also shows that H5N1 viruses are becoming increasingly pathogenic in animals than earlier H5N1 types (CDC, 2014). Other subtypes of avian influenza virus also have infected in birds. Among them the most frequently detected subtype is H9N2 (FAO, 2014).

Different methods have been designed and developed for detection of avian influenza, such as electrochemistry, and surface plasmon resonance, quartz crystal microbalance. Reverse transcription-polymerase chain reaction (RT-PCR) provide high sensitivity and fast detection time, but are limited by the high cost, complicated procedure and requiring specialized laboratories and equipment (Ellis and Zambon, 2002). Another common method is the enzyme-linked immunosorbent assay (ELISA), which uses antibodies and color change to identify a substance. It has advantages such as its variety, fast and convenient, high sensitivity, but at the same time the cost of the monoclonal antibodies, unstable negative controls and the short term of the enzyme could limit the use of ELISA (Baker et al., 2009). A rapid and portable user-friendly detection system will help and improve the detection of AIV H5N1.

Impedance measurement detection is considered an effective and rapid detection option (Bai et al., 2012; Wang et al., 2013; Zhang et al., 2007). Moreover, an impedance detection device could be designed and fabricated in portable dimension and could be controlled by a laptop (Zhang et al., 2013). Moreover, the application of the flow cell reduces the sample volume

and provides fast reaction rates with the small chamber that covers on the interdigitated microelectrodes (Hong et al., 2009). However, these detection procedures still need well-trained lab technicians to operate the sample delivery process, since the sample volume could not be controlled accurately each time. Therefore, this study is to develop a sample delivering system that could be controlled by a laptop with a user friendly control panel. This system combines impedance measurement with micro-flow cell to form a completed portable detection system for AIV measurements.

LabVIEW is a software from National Instruments (Austin, TX) that can be used to create user friendly virtual instruments (VIs) on computers for measurement and control. With this software, virtual instruments were built for measurement, control, and data process. A VI has been made by Dr. Benhua Zhang for impedance measurement based on the audio card from a laptop. It has been proven that this VI impedance analyzer could qualify the work of impedance measurements for AIV detection (Zhang et al., 2013). Based on this work, a micropump and three valves are designed to work with a Data Acquisition (DAQ) to build a liquid delivery system connected to the flow cell. A separated VI has been programmed to control a flow cell system built for the sample delivery. Both the impedance measurement part and sample delivery part have been designed and packaged together, thus making it an integrated system for portable usage. The whole system is portable and easy to operate due to the laptop oriented design.

Chapter 2 Objectives

Avian Influenza H5N1 has been threatening human health and causing huge economic losses. Current methods for the detection of H5N1 required well trained personnel and lack portability. An impedance biosensor has been developed in which LabVIEW was used to build the virtual impedance analyzer to provide the portability. The goal of this study was to develop a portable and automated impedance biosensing system by integrating laptop-based impedance measurement, interdigitated microelectrode in a microflow cell, sample delivery with virtual instrument for in-field rapid detection of AIV H5N1.

The specific objectives of this project were as follows:

1. To design and fabricate the integrated biosensing system containing impedance measurement, interdigitated microelectrode in a flow cell, and sample delivery with virtual instrument.
2. To evaluate the biosensing system for its accuracy and reliability in impedance measurement by comparison with a commercial impedance analyzer.
3. To evaluate the biosensing system for its sensitivity and specificity with the tests on different concentrations of AIV H5N1 and non-target AIV subtypes.

Chapter 3 Review of the Literature

3.1 Influenza A Virus H5N1

Influenza A viruses together with Influenza B viruses and Influenza C viruses comprise the family *Orthomyxovirida*, among them only Influenza A genus are known to infect birds (Thomas and Noppenberger, 2007). Influenza A viruses have a helical capsid surrounded by a lipoprotein envelope and consist of a single stranded negative sense RNA genome segmented into 8 fragments (Lee and Saif, 2009). A lipoprotein covers the nucleocapsid and consists of a lipid layer interspersed with membrane proteins, and can occur in either spherical or helical forms (Jin et al, 1997). The dimensions of the virus particles are dependent on their special shapes. For spherical particles they are usually 50-120 nm in diameter while for filamentous particles they are 20 nm in diameters and 200-300 nm in length. Influenza A virus has a high mutation rate of 1/10000 because of the use of RNA instead of DNA and the use of RNA dependent RNA transcriptase (Chen and Holmes, 2006).

Based on the antigenic relationships in the surface glycoproteins haemagglutinin (HA) and neuraminidases (NA), influenza A viruses can be classified into different subtypes. There are 16 HA subtypes and 9 NA subtypes. According to these surface glycoproteins in influenza viruses, certain names are given to the viruses such as H5N1. These two surface glycoproteins are functional for the infection of host cells with haemagglutinin binding to sialic acid receptors at the cell surface and neuraminidase catalyzing the cleavage of virus particles from the sialic acid sites on the host cell (Wong and Yuen, 2006). Although influenza A viruses with H1-H3 and N1-N2 can cause human infections, other subtypes have been identified responsible for human infection as the first case of H5N1 infection in 1997 in HongKong (Amano and Cheng, 2005). In another classification, based on the virulence, the influenza A viruses can be classified into two groups: one is called low virulence viruses (LPAI) and the other one can cause highly

pathogenic avian influenza (HPAI) limited to subtypes H5 and H7. Avian influenza virus subtype H5N1 is one of the HPAs and can infect domestic poultry and even humans by close contact (Fang et al., 2008).

Aquatic birds are believed to serve as the natural reservoir for avian influenza A viruses. The H5N1 viruses are transmitted through the saliva, nasal secretions and feces of infected birds and other birds could be infected through close contact with these excretions. Considering the migration of these infected birds, it could spread to the whole world. In cases of human infection of H5N1, those reported cases have approximately a 60% mortality rate, although it is believed that still a certain number of cases of H5N1 infection go unreported (Thorson et al., 2006).

Most previous outbreaks of avian influenza originated in southeast and east Asia. In these places it is usually crowded with humans, poultry and livestock. Viruses have more chances to mutate into a subtype that more easily infects humans in these conditions. The process that the viruses move from wild birds to domestic animals and humans can be termed as host-adaptation. Study shows that the amino acid and RNA codon sequences could determine the possible mutations in H5N1 hemagglutinins (Wu and Yan, 2006). Although it is not confirmed that H5N1 could spread among human, human to human transmission exists according to several cases in Sumatra in 2006 (Lauerman et al., 2006; Jones et al., 2006)

Avian Influenza H5N1 threatens not only the human life but also the world economic. The loss of birds and necessary quarantine procedures to control further infection of the viruses greatly influence the poultry industries (Burns et al., 2008). A culling and vaccination method has been applied to control the spread of influenza with 35 million birds having been killed,

causing huge economic loss and 55 billion vaccinations administered by government financial support since 2004 (Chen, 2009).

3.2 Current Methods of H5N1 Detection

Since the outbreak of avian influenza virus could bring huge loss of human life and high cost worldwide, it is essential for controlling the spread and outbreak by early identification of avian influenza viruses (MacKay et al., 2008). Different methods have been developed for avian influenza. Some currently used methods for influenza detection include viral isolation culture, direct immunofluorescent assay, immunochromatographic strips, enzyme-linked immunoassay, complement fixation, hemagglutinin-inhibition, and reverse-transcription-polymerase chain reaction (Amano and Cheng, 2005).

Compared to all other virus detection methods, viral isolation culture with immunological antigen conformation is the gold standard technique (Leland and Ginocchio, 2007). The first step of viral isolation for influenza viruses is to inoculate specific pathogen-free embryonated chicken eggs or cell cultures with a virus sample, thus allowing the virus infectivity to be measured in either 50% Egg Infectious Dose per ml (EID₅₀/ml) or 50% Tissue Culture Infectious Dose per ml (TCID₅₀/ml). For subtyping of the virus, hemagglutinin-inhibition is performed, which is based on antibody binding of hemagglutinin hindering the ability to agglutinate of erythrocytes. Viral isolation is still not considered as an efficient detection method since the long incubation times, specialized eggs or cell cultures and high level of technical expertise, even though it is inexpensive and can provide excellent sensitivity (Charlton et al., 2009).

Unlike the viral isolation, molecular detection methods are not limited by cell cultures, long incubation times and high level expertise. Among the molecular methods, reverse

transcription-polymerase chain reaction (RT-PCR) offers both high sensitivity and fast detection time. In order to determine the phylogeny of a virus the segments of viral RNA is amplified by RT-PCR for isolation and identification. Reverse transcriptase is used to convert the RNA genome segments into DNA copies (cDNA) because DNA is needed for PCR amplification. Following the enzyme polymerase is used to amplify the cDNA segments. As the starting point for DNA replication, DNA primers can pick a certain region of the hemagglutinin gene for the detection of a specific influenza gene (Dawson et al., 2007). Another related method is the real time RT-PCR technique which is a developed version of RT-PCR that it detects the specific gene fragments using fluorescent probes while operating the gene amplification. The real time RT-PCR technique has better specificity than the traditional RT-PCR because of the specific designed probes for the certain sequence of DNA. Moreover, the real time RT-PCR method supports simultaneous multiple gene detections. Although RT-PCR has the advantages of rapid detection, good specificity and sensitivity, it is still limited by the high cost, requiring specialized laboratories and equipment, high false positive rates and the complicated procedure (Ellis and Zambon, 2002).

Compared to viral isolation and RT-PCR, immunochromatographic strips are a simpler detection method. The principle is that the enzyme-labeled antibodies bound to a membrane and reagents are used to cause a color change on a strip signifying the presence of virus. The tests can be easily performed within half an hour, though subtype information are not offered and the sensitivity is low (Marandi, 2010).

3.3 Biosensors

The concept of biosensor was first developed by Leland C. Clark in 1962 with his enzyme microelectrodes. Following this many other biosensors with different properties were studied and developed by other scientists and research institutes from different fields (Mohanty and Kougiannos, 2006). As combined with the modern information technology, the biosensor technique offers the possibility for rapid, sensitive and real-time measurements for microbial detection (Seo et al., 1998).

A biosensor can be described as a device that consists of three parts: biological element, transducing element, and a signal processing element. A more detailed definition of biosensor made by The International Union of Pure and Applied Chemistry is “a device that uses specific biochemical reactions mediated by isolated enzymes, immunosystems, tissues, organelles or whole cells to detect chemical compounds usually by electrical, thermal, or optical signals” (IUPAC, 2006). The biological sensing of a biosensor might be enzymes, antibodies, cells, organelles or tissue, while the transducer might consists of parts that are electrochemical, optical, acoustical or mechanical (Turner et al., 1987). Biosensor technology has been applied in environmental, mining, food and drug analysis, and processing control for its advantage of versatility. As the application of biosensors expanding, modified biosensors have been developed, which are based on analysis of refractive index change, measurement of mass, measurement of fluorescent or luminescent emissions, and a diverse range of colorimetry, electrochemical, charge, mass and spectral effects (Hall, 2002). Compared to the conventional methods, the new developed biosensors have higher specificity, faster reaction time and more sophisticated data processing method.

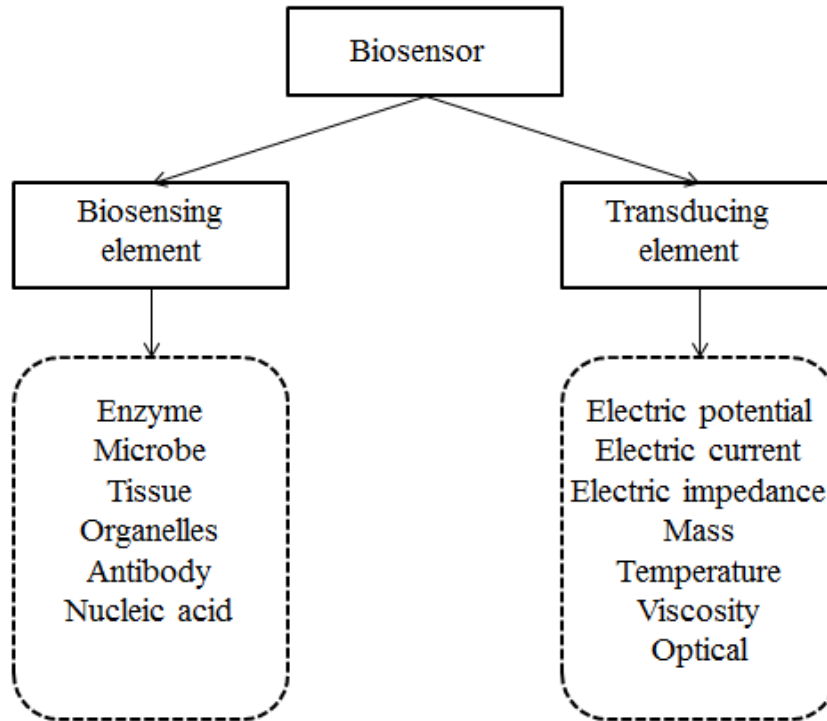


Figure 3.1 - Elements of a biosensor

3.3.1 Major Types of Biosensors used in Microbial Detection

The biosensors applied in the area of microbial detection may be classified into three main types: optical, piezoelectric and electrochemical.

The principle of optical biosensors is using visual phenomenon to show the interaction between the target analyte and the biological probe of the biosensor. Biosensors using this principle are fluorescent sensors, absorption, luminescence and surface plasmon resonance (SPR) sensors. The change of the color may be trigger in two ways in an optical biosensor: either the optical properties are directly changed by the analyte or through a label tagged with the analyte. Based on this, the optical biosensors can be divided into two categories: requiring labels or label-free optional biosensor. One example for the label required optical biosensor is the fluorescence biosensors, whose labels are usually dyes, quantum dots and fluorescent proteins (Medintz et al.,

2005). Unlike the fluorescent biosensors, label-free optical biosensors require fewer steps and give correct positives and negatives (Cooper, 2002). SPR biosensor is one of the label-free optical biosensors, which measures the change in refractive index and is effective real-time detection of bacteria, viruses and proteins (Philips and Cheng, 2007).

3.3.2 Impedance Measurement and Impedance Biosensors

Impedance is an expanded concept of resistance. It can be represented as a complex number consisting of the frequency independent part called real part R and the frequency dependent part called imaginary part X . The imaginary part is reactance which is affected by the capacitance and inductance and varying with the change of the frequency of the current passing through. Increasing frequency will increase the impedance due to inductance but decrease the impedance due to capacitance. Usually the inductance in electrochemical measurements is negligible.

Nyquist plot or Bode plot are usually implied for impedance data presentation. For measuring Faradic impedance, Nyquist plots are used which shows the real part versus the imaginary part in an X-Y graph. In non-Faradic impedance measurement the Bode plot is the preference which shows the log of the frequency (X axis) versus the log of the impedance magnitude and the phase angle shift (Y axis) (Barsoukov and Macdonald, 2005).

The following formulas show the basic calculation in impedance measurement. First is the calculation for the impedance magnitude:

$$|Z| = \sqrt{R^2 + (X_L - X_C)^2} \quad 3.1$$

Where \mathbf{R} is the resistance, \mathbf{X}_L is the impedance due to inductance which is negligible in electrochemical measurements, \mathbf{X}_C is the impedance due to capacitance, which can be calculated using the formula:

$$\mathbf{X}_C = \frac{1}{2\pi f C} \quad 3.2$$

Where f is the frequency in Hz and C is the value of the capacitor in F. The phase angle is calculated by the formula:

$$\varphi = \tan^{-1} \left[\frac{X_L - X_C}{R} \right] \quad 3.3$$

Impedance biosensors use a sinusoidal voltage within a certain frequency range or a given frequency to measure the impedance under constant DC bias conditions (Daniels and Pourmand, 2007). This can be done with the help of a probe that captures the target molecule, thus stabilizing them. These biological sensing probes consists of different elements among which antibodies are the most commonly used, while other materials such as aptamers are widely used for impedance biosensor probes. It has been proven that impedance biosensors are qualified in detecting eukaryotic cells, bacteria and viruses (Varshney and Li, 2009; Wang et al., 2009; Houssin et al., 2010). Impedance biosensors have the advantages of low cost, mobile detection and user-friendly operation, which can optimize many tests for infectious pathogens. Moreover, impedance biosensors can be combined with other technology such as magnetic separation techniques to enhance the efficiency for detection of pathogens from blood, food or environmental samples (Ivnitski et al., 1999).

3.3.3 Aptamers

Aptamers are artificial designed molecules of oligonucleic acid or peptide, which can bind to specific targets such as drugs, amino acids, cells and viruses with high affinity and selectivity (Jayasena, 1999). With this property, aptamers could be a reliable alternative for antibodies in many applications. The Gold lab (Tuerk and Gold, 1990) and the Szostak lab (Ellington and Szostak, 1990) are the two labs that first develop the aptamers in 1990 in the USA. Usually the specific aptamers are selected from a large random oligonucleotide pool which is called Systematic Evolution of Ligands by Exponential Enrichment (SELEX), while the natural aptamers also exist in riboswitches. Aptamers can be classified into DNA or RNA or XNA aptamers (consist of strands of oligonucleotides) and peptide aptamers (consist of a variable domain). Aptamers offer a good choice in both research area and clinical cases.

Compared to monoclonal antibodies, aptamers show a higher affinity to the targets (Jenison et al., 1994). Although aptamers are similar to antibodies in the variety of applications, several advantages are possessed by aptamers, such as self-refolding, single chain and redox-insensitive, easier and more economical to produce (Stoltenburg et al., 2007). Other advantages of aptamers over antibodies will be higher thermal stability, artificial designed and modified, longer shelf life (Sefah et al., 2009). Aptamers have been successfully used in many research cases for its advantages over antibodies. Bai et al. (2012) used the aptamer to develop an aptamer based SPR biosensor for the detection of AIV H5N1 with the lower detection limit of 0.128 HAU.

3.4 Interdigitated Arrays Microelectrodes (IDAM) Based Impedance Biosensors

IDAM as an element for portable impedance detection has been increasingly used for detecting microbial pathogens. Unlike the conventional microelectrodes such as thin metal rods or wires, IDAM has higher detection sensitivity, requires less volume of samples and shorter detection time (Towe and Pizziconi, 1997). Due to the design of the IDAM within a flow cell, the surface to volume ratio increases which at the same time decreases the distance for the conductive ions diffuse to reach sensor surface, resulting in a shorter detection time and minimizing the noise from non-target analytes (Kim et al., 2004). The system configurations of IDAM for impedance detection are classified into two categories: open and close chip. Open chip configurations are simpler and can be used to improve the conventional impedance detection, while close chip configurations are embedded into a flow cell connected to microchannels. These two configurations have been used in many cases which are all related to direct and indirect impedance measurement and dielectrophoresis (Gomez et al., 2002; Suehiro et al., 2003; Radke and Alcocilja, 2005).

3.5 Microfluidics

The microfluidics is used to design systems that can handle small volumes of fluids. Microfluidics was used in DNA chips, lab-on-chip (LOC) technology, micro-propulsion, and micro-thermal technologies (Wikipedia, 2014). At the microscale the behavior of fluids will differ from that at macroscale in factors like surface tension, energy dissipation and fluidic resistance can dominate the system (Karniadakis et al., 2005). The microfluidics can be used for pathogen detection. Ultrafast rRT-PCR detection of avian influenza has been conducted by using the microfluidic droplets (Pipper et al., 2007). A method based on microfluidic was developed

for detection of malaria in field (Lee et al., 2010). For the application on LOC devices, Lee et al developed a LOC that could perform RT-PCR for rapid detection of AIV and Huh et al. built a LOC for the detection of severe acute respiratory syndrome (SARS) virus (Lee et al., 2008; Huh et al., 2008). Microfluidics can reduce the detection time, increase efficacy of detection antibodies in immunosensors provide and have a high surface to volume ratio (Bange et al., 2005; Ohno et al., 2008).

3.6 LabVIEW Software

LabVIEW is a programming platform from National Instruments (Austin, TX) that can create virtual instruments (VIs) on computer for measurement and control and is designed for use in almost all industry area. Unlike the traditional programming language, LabVIEW is graphical based programming language, acquiring data sending out orders through the Data Acquisition (DAQ). A typical LabVIEW program is written using icons which are packaged functions, like the class in C++. These icons are placed and wired up by the programmer and these wires show the data flow from icon to icon. There are other programming languages sharing the visual programming concept, such as Visual Basic, but it still needs some coding parts.

LabVIEW consists of two major working interfaces for the programmer: block diagram and front panel. The block diagram is the place where the programmers can place the icons and wire them together, which is similar to a circuit diagram. The data will flow from left to right along the wires through different icons which have certain functions. For example, usually the icon that represent the data collection parts are located in the far left and the right edge is the icon for final data output. While the program is being executed, the user cannot manipulate the block diagram but only the front panel. The front panel is the user interface of the VI, which

consists of different elements such as numerical indicators, control buttons or knobs and graphs, which is like the control panel on any physical electronic equipment.

The palettes are the tools for the programmer to use and build the block diagram and front panel. It consists of three parts: tools, controls and functions palettes. Programmers can find the specific icons and indicators for editing the block diagram and front panel and these operations can be easily done by clicks on the icon of the control and the places it will be put. The tools palette is for user to change the mouse cursor into different modes. The controls palette is for editing the front panel and the functions palette consists of all the icons for program the block diagram. These functions might be logical loops, mathematical operations and file operations (National Instrument, 2012).

Chapter 4 Materials and Methods

4.1 Materials

4.1.1 Biological and Chemical Reagents

The Millipore water purification system (Mill-Q, Bedford, MA) provided all the water used in this study. Phosphate buffered saline (PBS, 10X) was purchased from Sigma-Aldrich (St. Louis, MO) and diluted with Milli-Q (Mill-Q, Bedford, MA) water to 10 mM (pH 7.4) for use in all tests. Streptavidin was purchased from Rockland Inc. (Gilbertsville, PA) and reconstituted in 10 mM PBS and stored in 1 mg/ml aliquots at -20 °C.

Inactivated avian influenza subtypes H5N1 (Scotland/59) was provided by the USDA/APHIS National Veterinary Services Lab (Ames, IA), which were inactivated by the providers using β -propiolactone, eliminating infectivity while preserving hemagglutination activity (Goldstein and Tauraso, 1970). The stock concentration of viruses was 2^7 hemagglutination units (HAU) $50 \mu\text{l}^{-1}$. Sterile PBS (10 mM, pH 7.4) was chosen for diluting the virus. Subtypes such as H1N1 H5N2 H5N3 were all killed and obtained from Animal Diagnostic Laboratory at Penn State University, University Park, PA. These subtypes were prepared for specificity tests.

The AIV H5N1 aptamer (73 nucleotides; 5'-GTG TGC ATG GAT AGC ACG TAA CGG TGT AGT AGA TAC GTG CGG GTA GGA AGA AAG GGA AAT AGT TGT CCT GTT G-3') was developed in our group with detailed information described in our previous study (Wang et al., 2013). The aptamer was synthesized and biotin labeled by Integrated DNA Technologies (Coralville, IA). It was diluted using PBS to a working concentration of 0.023 mg/ml and stored at -20 °C.

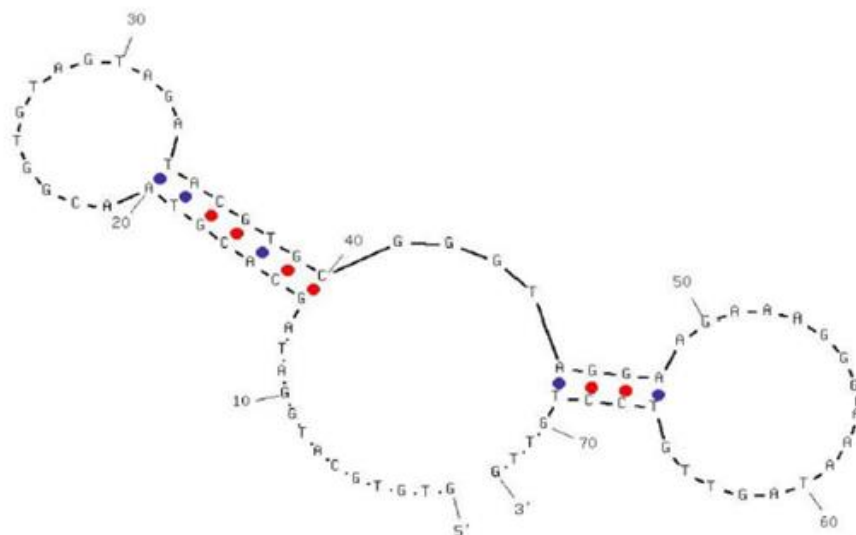


Figure 4.1 – Secondary structure of the H5N1 aptamer (Adopted from Wang and Li, 2013).

4.1.2 Interdigitated Array Microelectrodes and Flow Cell

The Institute of Semiconductor of Chinese Academy of Sciences, Beijing, China, fabricated the interdigitated array microelectrodes by depositing a 100 nm-thick layer on a glass wafer using a 10 nm thick layer of chromium as adhesion layer and patterned by photolithography. Each IDA microelectrodes includes 25 pairs of digit microelectrodes with 15 μm digit width, 15 μm inter-digit space and 3 mm digit length. The working area of the IDAM was 4.5 mm^2 , while the total area of the IDA microelectrodes was 77 mm^2 . The flow cell used in this study was made of PDMS, fabricated by Dr. Tiemin Zhang at South China Agricultural University, Guangzhou, China (Zhang and Li, 2013). The dimension of the flow cell is 60 x 47 x 74 mm (W x H x D) and it had a microchamber of 8.7 mm^3 and two microchannels with 1mm diameter (Wang et al., 2014).

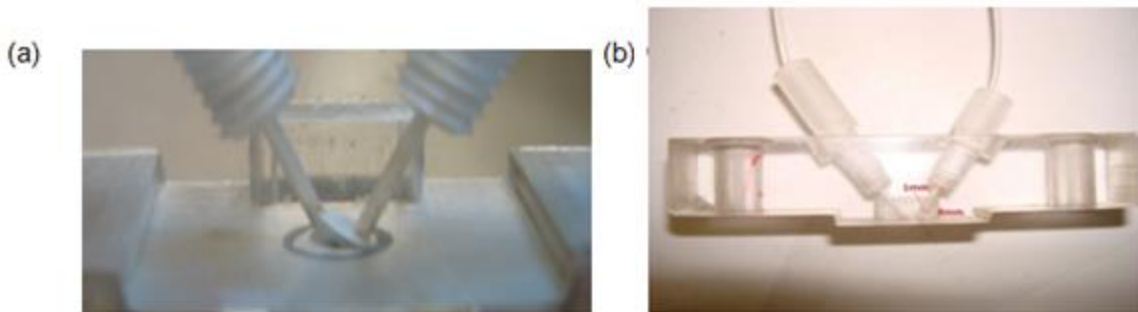


Figure 4.2 - (a) The front view of the flow cell and (b) the microchannels for sample delivery (diameter: 1mm, length: 8 mm) (Zhang and Li, 2013).

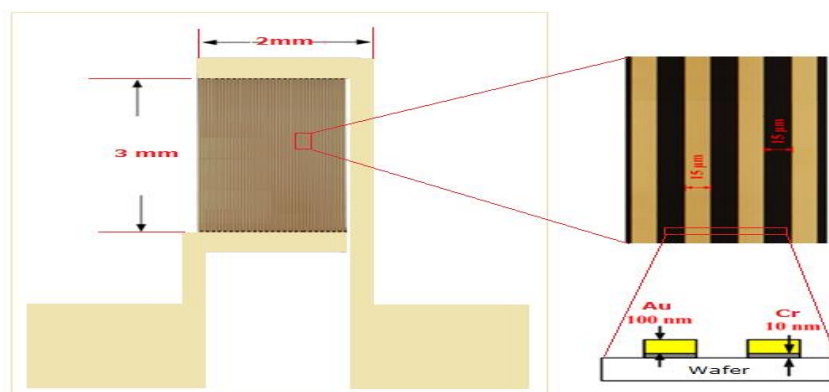


Figure 4.3 - Gold interdigitated array microelectrode.

4.1.3 Pumps and Valves

SP 100 series pump was purchased from APT Instruments (Litchfield, IL). It was powered by 12 Vdc, 75 to 300 mA with adjustable rotation speed. The dimensions (W x H x D) was 60 x 47 x 74 mm. The accuracy and repeatability of the pump were both $\pm 10\%$ full scale. Tubing dimension, fluid viscosity and back pressure would influence the flow rate. The 120Sp series valve was purchased from Biochem Fluidics (Boonton, NJ) with dispense volume 20 μ l. The body and diaphragm of the pump were made of phenylene sulfide and ethylene propylene diene monomer, respectively. The operation voltage of the pump shared the same 12 Vdc as the pump.

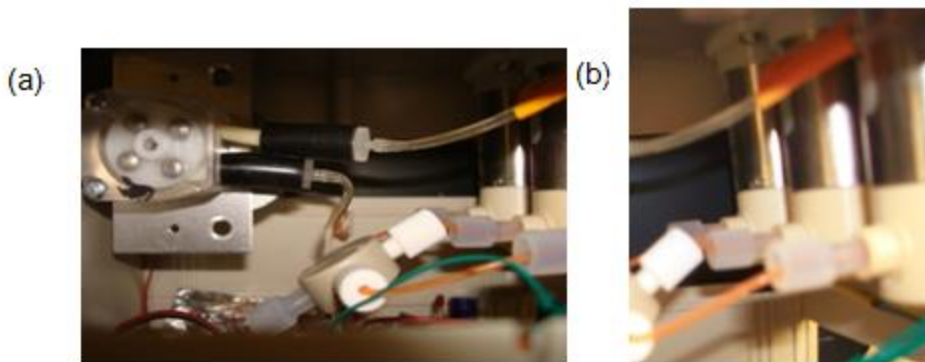


Figure 4.4 - (a) The SP 100 series pump and (b) 120 SP series valves connected to tubings.

4.1.4 Laptop and DAQ

The core data processing part of this system is the laptop. In this study, Dell Latitude E6430 was selected with LabVIEW 2012 installed. The operation system installed was Windows 7 –64bit. The Data Acquisition card was USB-1208fs purchased from Measurement Computing Corporation (Norton, MA).

4.2 Detection of AIV H5N1

4.2.1 Pretreatment of Microelectrodes

The interdigitated array microelectrodes were first cleaned by 30 μ l NaOH (1mol) for 10 min then washed with deionized water. Then the microelectrodes were dried first by the lens cleaning paper and nitrogen. Following this the microelectrodes were washed with 20 μ lHCl (1mol) using the same protocol.

4.2.2 Impedance Measurement

The impedance measurements were conducted by both the developed virtual instrument and the standard physical instrument IM6 impedance analyzer for a comparison study at 108 Hz.

The virtual instrument was originally designed by Dr. Benhua Zhang (Zhang et al., 2013) and it used the laptop's audio card to perform the frequency scanning as the excitation signal. The frequency range of this virtual instrument was 60 Hz to 200 Hz (Zhang et al., 2013).

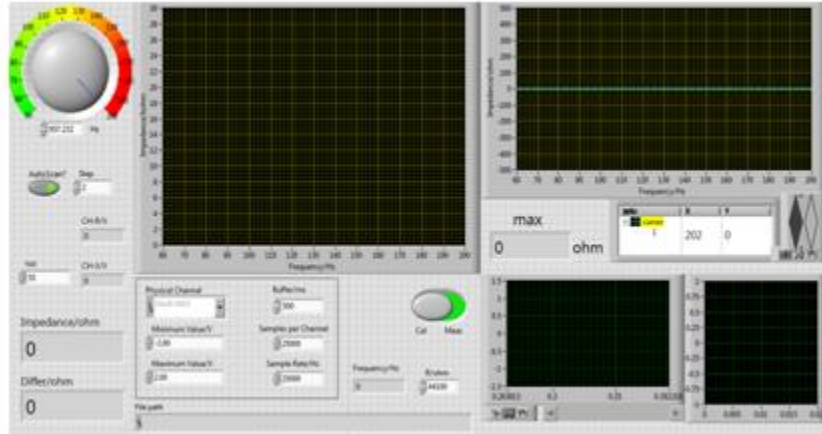


Figure 4.5 - The virtual impedance analyzer developed in LabVIEW (adopted from Zhang et al., 2013).

The structure of the virtual impedance analyzer is shown as following:

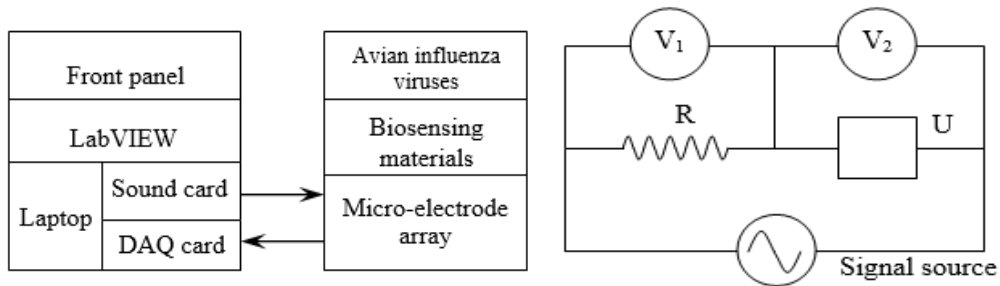


Figure 4.6 - (a) The structure and components of the virtual impedance analyzer and (b) the circuit of measurement (Adopted from Zhang et al., 2013).

$$I = \frac{V_1}{R} \quad 4.1$$

$$Z = \frac{V_2}{I} = \frac{V_2}{V_1/R} \quad 4.2$$

The excitation signal was generated by the audio card of a laptop. The U is the unknown unit which is the detection target, and the R is resistor in the measurement circuit. After the voltage

value V_1 and V_2 were measured by LabVIEW through the DAQ, the impedance value of the target U could then be calculated by the equation 4.1 and 4.2.

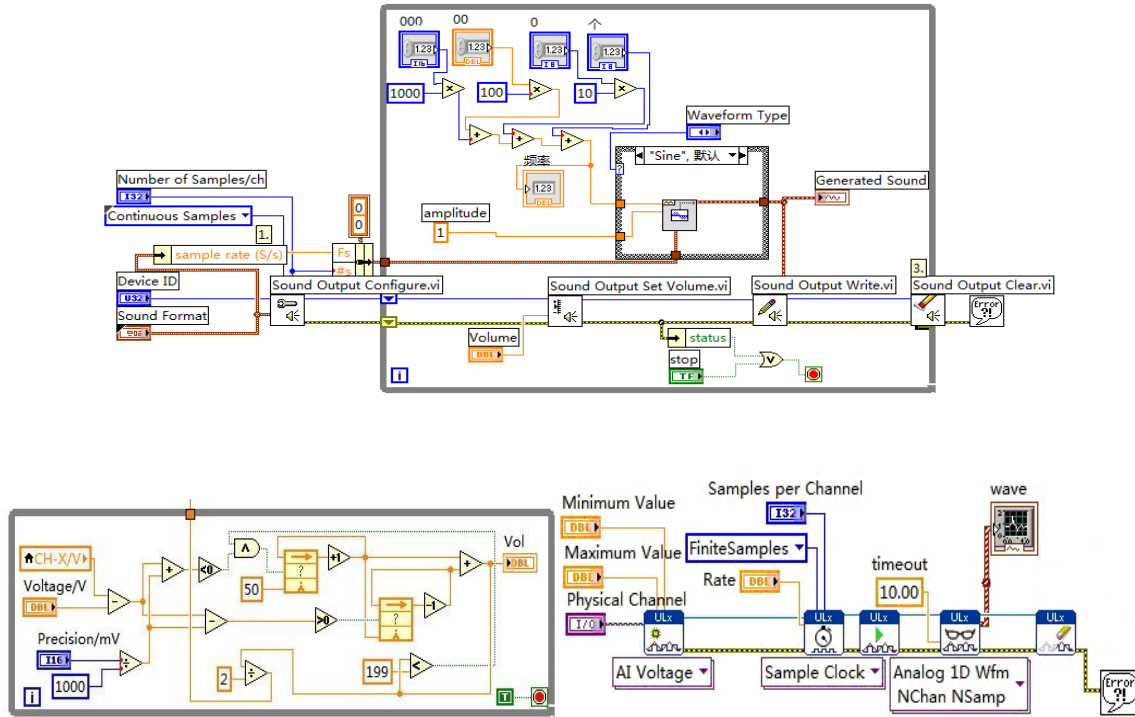


Figure 4.7 – Block diagram design of the virtual impedance analyzer (Adopted from Zhang et al., 2013).

The IM-6 impedance analyzer (BAS, West Lafayette, IN) with IM-6/THALES software was used for the comparison study. Unlike the virtual instrument, this standard physical impedance analyzer could record a Bode diagram (impedance and phase vs frequency) and has a wider frequency range (1 Hz to 100 MHz) with an amplitude of 5 mV.

4.3 Working Procedure of the Biosensing System

First step was to clean the IDMA and stabilize it into the flow cell for test. Next the sample delivering system was started with first opening valve 1 for 55 s to deliver the

streptavidin solution to the chamber. After 45 min, the impedance value was measured both by IM6 impedance analyzer and VI impedance analyzer. The following step was pumping the aptamer solution into the chamber through valve 2 for 55 seconds, after which 45 min incubating time was needed and the impedance was measured in the same way in last step. Next, the system delivered the sample solution into the chamber with another 45 min incubation before the impedance measurements. Finally, the pump worked on washing mode for 5 min to finish the task, with valve 1 being connected to dH₂O. By changing the hardware setup, the system could tune the flow rate of the washing mode within the flow rate limit.

Chapter 5 Results and Discussion

5.1 Design and Fabrication of the Biosensing System

The whole system was divided into two parts to design and fabricate: software and hardware. The software section contained the virtual instruments for impedance measurement and also controlled the sample delivery system. Then, the hardware system was designed according to the LabVIEW program and the parameters of those parts purchased. At the same moment, the software needed to give compromise to the limitation of the hardware (Wang et al., 2014). Below is the structure of the system:

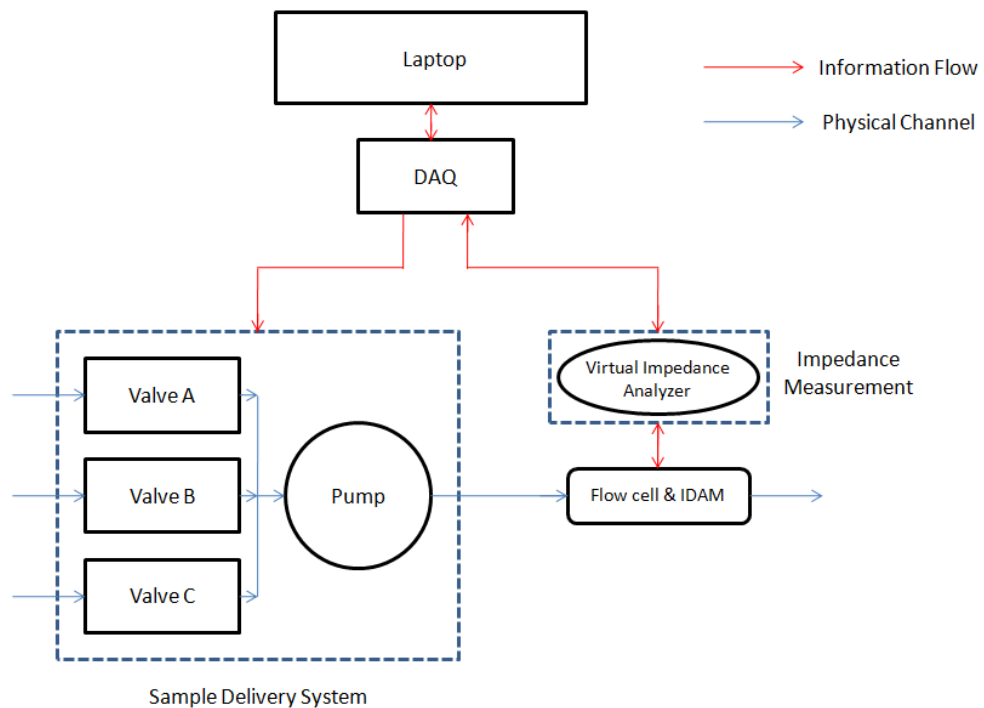


Figure 5.1 - Structure of the biosensing system.

5.1.1 Software Design and Fabrication

The control system of this flow system was designed in LabVIEW as a virtual instrument (VI) working with a Data Acquisition (DAQ) to control the pump and valves. Certain codes had been programmed for the sequential procedure and different flow rate options. The flow rate could be adjusted by tuning the circuit, with a range from 170 $\mu\text{l}/\text{min}$ to 545 $\mu\text{l}/\text{min}$ tested in a 0.8mm tubing. Sequential controlling method was programmed into a VI by LabVIEW. Parameters for controlling the delivering system could be set on the front panel and remaining time is shown on the right side, respectively. A front panel was designed for the users to set the timing parameters for sample delivery.

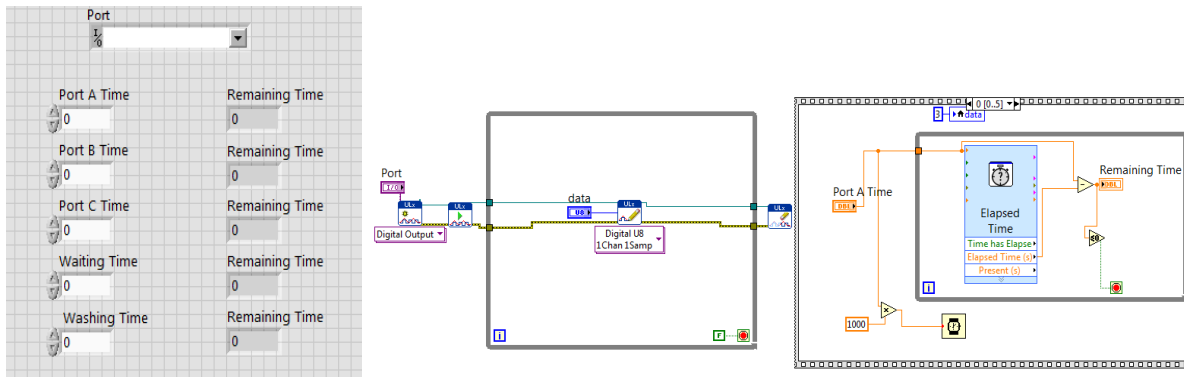


Figure 5.2 - (a) Front panel design and (b) block diagram of the virtual instrument for control.

As shown in figure 5.2, the front panel and block diagram were designed in LabVIEW for controlling the sample delivery system. In the front panel, a port selection window was for the user to set the working port on the DAQ and three data lines were designed to control the three input ports: A, B and C. User could type the time in seconds on in front panel to control the working time for each input ports, the waiting time after each step and the washing time at the end of a recycle. The value in those Remaining Time windows could not be changed by user and they were designed to show the remaining time of each step. In the block diagram, two types of

logical structures were implied as the main structure. The first while-loop (a logical programming structure in LabVIEW) on the left was used to send control data through the DAQ to the pump and three valves. Next, the sequence structure functioned for the sequential controlling, which meant that every signal sent to the DAQ had to follow a certain order. Inside the sequence structure, another while-loop was drawn for updating the remaining time windows. ULx library from measurement computing (Norton, MA) was used for writing the data flow to the DAQ.

The output control signals were coded in binary format, which would drive the DAQ to control the valves and pump. Below is the detail control method:

Table 5.1- Sequential Control of the sample delivering system.

Control Code	Mode	Note
1xxx	Speed 1	Valves working under speed1
11	Open Inlet 1	Close valve 2 and 3
101	Open Inlet 2	Close valve 1 and 3
1001	Open Inlet 3	Close valve 1 and 2
1xxx0	Speed 2	Valves working under speed 2
11000	Washing Mode	Washing speed option

These control codes were packaged in the block diagram which could not be accessed by the user, so they were not needed to be remembered.

5.1.2 Hardware Design and Fabrication

The hardware parts were packaged into a project box. Inside the box, a DAQ and a cut bread board were set with other electronic parts such as relays and resistors. A 110VAC-12VDC

cord powered the whole system and two adjustable resistors supplied the different speed options of the pump. By using the control codes in table 1, the different speed mode of the pump could be selected. As shown in figure 5.3, three inlets were connected to valve A, B and C, respectively, then the three valves were connected to the inlet of the pump after which would be the inlet of the flow cell.

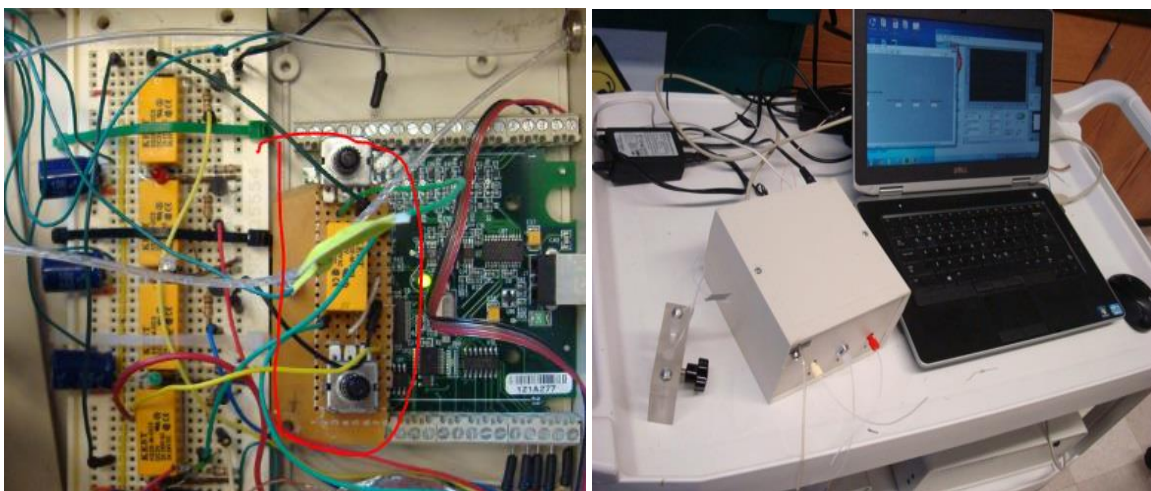


Figure 5.3 - (a) Circuit design of the sample delivery system and (b) the whole hardware system

As shown in figure 5.3, the control circuit used the DAQ as the bridge for the data communication between the laptop and the pump and valves. The virtual instrument developed in LabVIEW first sent out the orders to the DAQ, then the DAQ would process and convert them into analog or digital signal format, according to different ports. Next these orders would trigger the relays which worked like switches to control the pump and valves. Two adjustable resistors could tune the speed of the pump for washing mode and sample delivery mode. The detailed control method was shown in Table 5.1.

5.2 Comparison of the Impedance Measurements

Impedance was measured after each layer was immobilized on the interdigitated array electrodes by both virtual instrument and IM6 impedance analyzer for a comparison. In total there were four impedance curves for one microelectrode: bare microelectrode with redox, redox/streptavidin, redox/streptavidin/aptamer/blocking solution, and redox/streptavidin/aptamer/H5N1 sample. The impedance measurements for each layer were first conducted by the IM6, following by the virtual instrument. Although the time difference of the measurements could influence the results, it could be ignored considering the error was not significant. Three microelectrodes were used for repeat test. Figure 5.4 shows the impedance measurement results of the three microelectrodes. The concentration of the H5N1 sample used in this test was 8 HAU and the frequency range of the curve was 60 Hz to 200 Hz for the virtual instrument and 50 Hz to 220 Hz for the IM6 impedance analyzer. The graph shows good consistency between the curves from the virtual instrument and the IM6 impedance analyzer. Even though at several frequency points the values are not matched well, overall they are still good expected results for the virtual instrument. The three microelectrodes had the similar results with detailed data in Table 5.2, which could prove the repeatability of the test. Take the first microelectrode as an example, (a) and (b) were the impedance of microelectrode 1 measured by virtual instrument and IM6. Both of them show the decreasing impedance curves for four layers as the frequency increasing. Moreover, the impedance change due to different layers immobilized on the microelectrode has the similar value. There are two significant impedance changes recorded by both virtual instrument and IM6: impedance change between bare microelectrode/redox and bare microelectrode/redox/streptavidin, impedance change between

bare microelectrode/redox/streptavidin/aptamer and bare microelectrode/redox/streptavidin/aptamer/H5N1 sample. The impedance change between bare microelectrode/redox/streptavidin and bare microelectrode/redox/streptavidin/aptamer was not obvious, which was also recorded by both the virtual instrument and IM6.

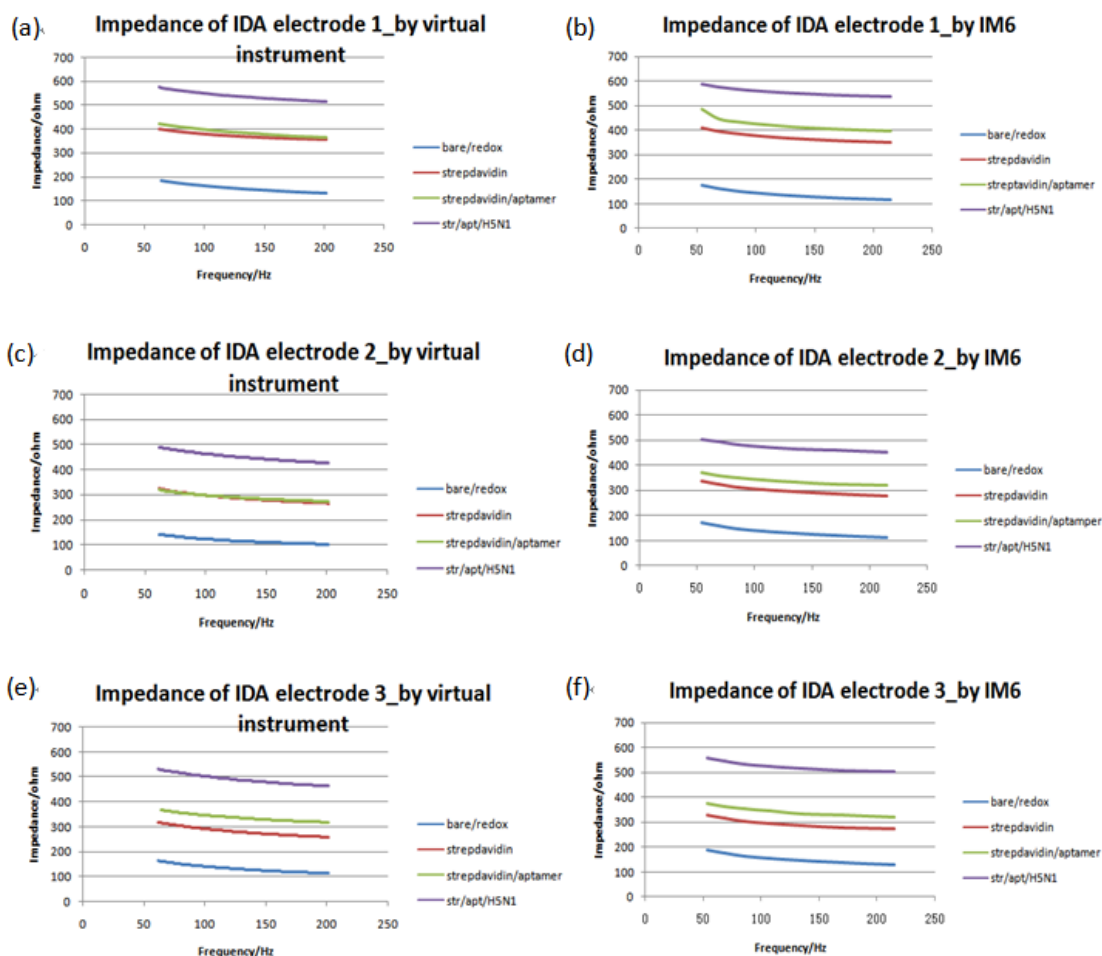


Figure 5.4 - (a), (c) and (e) Impedance measured from three IDA microelectrodes by IM6 and (b), (d) and (f) developed biosensor system. The H5N1 sample concentration was 8 HAU.

Since the commonly used stable frequency range using this detection protocol was around 100 Hz, a close frequency point 108 Hz was chosen for both virtual instrument and IM6 for comparison. In Table 5.2, the impedance values of each layer at 108 Hz were listed from both

virtual instrument and IM6. The mean impedance values of the three microelectrodes for each layer were calculated in the table, showing an error rate within 5%.

Table 5.2 - Impedance measured by IM6 and the developed biosensor system. The frequency point chosen was 108 Hz.

Electrode		Impedance value (ohm)			
Surface	Instrument	Microelectrode No. 1	Microelectrode No. 2	Microelectrode No. 3	Mean±S.D.
Bare microelectrode	IM6	140.7	138.4	154.7	144.6±8.8
	Biosensor	160.3	120.1	137.1	139.2±20.2
Streptavidin	IM6	375	302.4	295.8	324.4±43.9
	Biosensor	376.9	293.5	287.8	319.4±49.9
Aptamer	IM6	422.8	340.7	343.8	369.1±46.5
	Biosensor	394	294.4	342.7	343.7±49.8
AIV H5N1	IM6	556.8	474.1	524.8	518.6±41.7
	Biosensor	544.8	458.5	498.3	500.5±43.2

5.3 Specificity of the Biosensing System

Three other different subtypes of avian influenza viruses were used for evaluating the specificity of the biosensing system. Using the same IDA microelectrode preparation protocol, the final sample solution were replaced by H1N1, H5N2 and H5N3 because of their similar properties of the HA and NA proteins. Figure 5.5 shows the impedance change due the different subtypes sample solution. As shown in figure 5.5, with the same concentration which is 8 HAU for all the test objects, only H5N1 sample generates impedance change around 150 ohm, which is approximately 10 times to the impedance changes made by H5N2 and H5N3. The H1N1

sample causes a negative impedance change and the control group almost has not changed. 108 Hz is the corresponding frequency for the impedance changes.

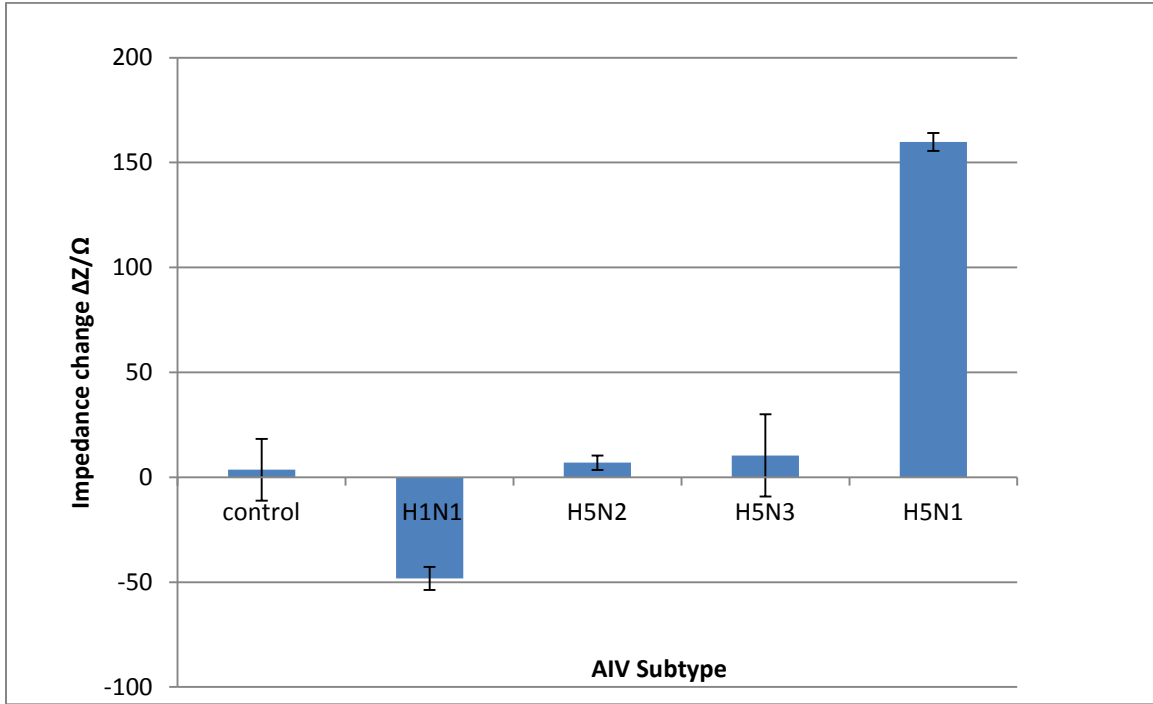


Figure 5.5 - Impedance changes at 108 Hz recorded by the biosensing system for the target H5N1 virus along with the three non-target AIV subtypes at 8 HAU. The means and error bars were calculated based on 2 replicates.

Table 5.3 - Impedance measured at 108 Hz recorded by the biosensing system for the target H5N1 virus along with the three non-target AIV subtypes at 8 HAU.

			Control	H1N1	H5N2	H5N3	H5N1
Impedance /ohm	Test 1	Blocking	384.6	384.6	384.6	384.6	294.4
		Sample	402.9	330.8	388.1	375.4	458.5
	Test 2	Blocking	302.2	302.2	302.2	302.2	342.7
		Sample	291.1	259.5	312.6	332.2	498.3
	Mean	Blocking	343.4	343.4	343.4	343.4	318.55
		Sample	347	295.15	350.35	353.8	478.4

5.4 Impedance responses to the different concentrations of AIV H5N1

Also, this biosensing system was evaluated by measuring different concentrations of AIV H5N1. The impedance changes at 108 Hz were chosen to evaluate the biosensing system because the frequency range around 100 Hz was considered to be the most stable area and 108 Hz was the closest frequency point we could find on the virtual impedance analyzer. From figure 5.6 it can be seen that the low concentration groups 0 HAU and 0.25 HAU are not obvious on the impedance change, though 0.25 HAU group does cause a little change on the impedance. As the concentration increased to 2 HAU, the impedance begins to change to around 90 ohm, which together with the 8 HAU and 16 HAU groups shows a good linear line. But the amplitude of impedance change decreased as the concentration increased to 16 HAU.

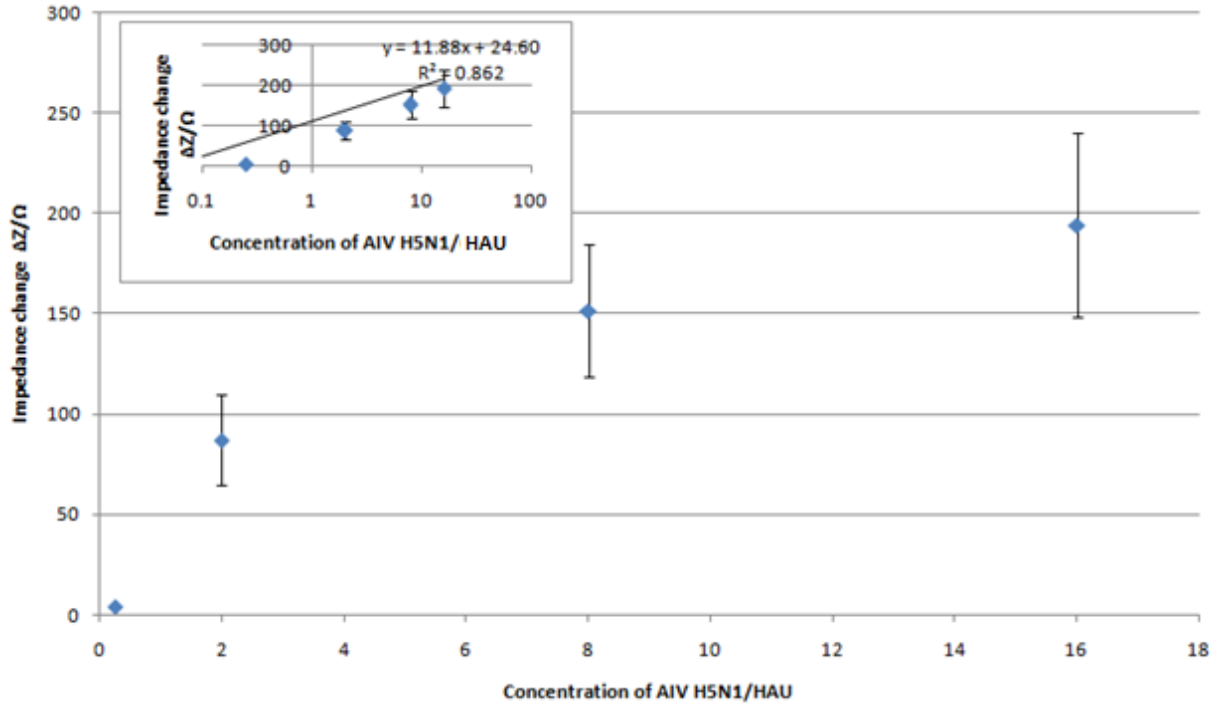


Figure 5.6 - Impedance changes at 108 Hz recorded by the biosensing system for different concentration of the target AIV H5N1 virus. The means and error bars were calculated based on 2 replicates.

Table 5.4 - Impedance measured at 108 Hz for different concentration of the target AIV H5N1 virus.

AIV H5N1 Concentration/HAU			0	0.25	2	8	16
Impedance /ohm	Test 1	Blocking	300.6	256.9	205.5	298.8	279.5
		Sample	298.8	260.8	270	483.6	519.8
	Test 2	Blocking	361.6	357.8	249.1	361.6	302.4
		Sample	358.9	362.3	358.8	480.1	450.8
	Mean	Blocking	331.1	307.35	227.3	330.2	290.95
		Sample	328.8	311.55	314.4	481.85	485.3

Chapter 6 Conclusions

A portable, automatic impedance biosensing system with a microfluidic cell and a pumping device was designed and fabricated for rapid detection of AIV H5N1 based on a laptop with LabVIEW. Sample delivery system could be controlled by the virtual instruments developed in LabVIEW for precisely delivering testing and washing solutions. Impedance could be accurately measured through the microelectrodes in the microfluidic cell using the sound card of a laptop with a DAQ card and then the data could be processed in the laptop. The developed biosensing system is simple and automated, and can better control the sample volume than manual operation. It could detect the H5N1 virus from at least other three subtypes: H1N1, H5N2 and H5N3. Also, this system could detect H5N1 at different concentration such 2 HAU, 8 HAU and 16 HAU, though it was designed just for showing positive or negative results. A linear relation between the concentration of AIV H5N1 and the impedance change was found for the calibration of the biosensing system in the range tested.

Chapter 7 Recommendations for Future Research

Further work on this study could concentrate on reducing the detection limit. This could be done with the improvements of the flow cell. Also, this system could only measure the magnitude of the impedance. If the phase angle could be measured in conjunction with the magnitude of the impedance, it would further perfect the whole system. Other improvements could focus on the updates of the hardware, such as replacing the DAQ, the pump and the tubing to achieve a better control precision. Also, adding the separation of target virus from samples to this system could further improve it.

References

- Amano, Y., & Cheng, Q. (2005). Detection of influenza virus: traditional approaches and development of biosensors. *Anal. Bioanal. Chem.* 381(1): 155-165.
- Bai, H., Wang, R., Hargis, B., Lu, H., & Li, Y. (2012). A SPR aptasensor for detection of avian influenza virus H5N1. *Sensors.* 12, 12506-12518.
- Baker G. B., Dunn S., Lajtha A., & Holt A. (2007). Handbook of Neurochemistry and Molecular Biology. Springer, New York. P. 215.
- Bange, A., Halsall, H. B., & Heineman, W. R. (2005). Microfluidic immunosensor systems. *Biosens. Bioelectron.* 20(12)2488-2503.
- Barsoukov, E., & Macdonald, J. (2005). *Impedance Spectroscopy: Theory, Experiment, and Applications* (2nd ed.). Hoboken, NJ: John Wiley and Sons.
- Burns, A., van der Mensbrugge, D., & Timmer, H. (2008). Evaluating the economic consequences of avian influenza. World Bank report. http://siteresources.worldbank.org/EXTAVIANFLU/Resources/EvaluatingAHIEconomics_2008.pdf. Accessed July 20, 2014.
- CDC. (2010). Key Facts about Avian Influenza (Bird Flu) and Highly Pathogenic Avian Influenza A (H5N1) Virus. <http://www.cdc.gov/flu/avian/gen-info/facts.htm>. Accessed May 18, 2014.
- CDC. (2014). Avian Influenza Current Situation. <http://www.cdc.gov/flu/avianflu/avian-flu-summary.htm>. Accessed May 18, 2014.
- Charlton, B., Crossley, B., & Hietala, S. (2009). Conventional and future diagnostics for avian influenza. *Comp. Immunol. Microbiol. Infect. Dis.* 32(4), 341-350.
- Chen, H. (2009). H5N1 avian influenza in china. *Sci. China C. Life Set.* 52(5), 419-427.
- Chen, R., & Holmes, E. C. (2006). Avian influenza virus exhibits rapid evolutionary dynamics. *Mol. Biol.* 23(12), 2336-2341.
- Cooper, M. A. (2002). Optical biosensors in drug discovery. *Nat. Rev. Drug Discov.* 1(7), 515-528.
- Dawson, E. D., Moore, C. L., Dankbar, D. M., Mehlmann, M., Townsend, M. B., & Smagala, J. A. (2007). Identification of A/H5N1 influenza viruses using a single gene diagnostic microarray. *Anal. Chem.* 79(1), 378-384.
- Ellis, J. S., & Zambon, M. C. (2002). Molecular diagnosis of influenza. *Rev. Med. Virol.* 12(6), 375-389.

- Ellington, A.D., & Szostak, J.W. (1990). In vitro selection of RNA molecules that bind specific ligands. *Nature* 346(6287), 818-822.
- Fang, L. Q., de Vlas, S. J., Liang, S., Looman, C. W., Gong, P., & Xu, B. (2008). Environmental factors contributing to the spread of H5N1 avian influenza in mainland China. *PloS One* 3(5), 2268.
- Goldstein, MA & Tauraso, NM. (1970). Effect of formalin, beta-propiolactone, merthiolate, and ultraviolet light upon influenza virus infectivity chicken cell agglutination, hemagglutination, and antigenicity. *Appl Microbiol.* 19(2):290-4.
- FAO. (2014). Action Plan on Emergency Response to Dangerous Avian Influenza Virus Strains with Potential Infection on Humans. http://www.fao.org/fileadmin/templates/faovn/files/Administration/ECTAD/MARD_action_plan_H7N9.pdf. Accessed May 18, 2014
- Hall, R. H. (2002). Biosensor technologies for detecting microbiological foodborne hazards. *Microbes and Infect.* 4, 425-432.
- Hong, J., Edel, J.B., & Demello, A.J. (2009). Micro and nanofluidic systems for high-throughput biological screening. *Drug Discovery Today.* 14, 134-146.
- Huh, Y. S., Park, T. J., Lee, E. Z., Hong, W. H., & Lee, S. Y. (2008). Development of a fully integrated microfluidic system for sensing infectious viral disease. *Electrophoresis* 29(14), 2960-2969.
- IUPAC. Compendium of Chemical Terminology, 2nd ed. (the "Gold Book"). Compiled by A. D. McNaught and A. Wilkinson. Blackwell Scientific Publications, Oxford (1997). XML on-line corrected version: [http://goldbook.iupac.org\(2006\)](http://goldbook.iupac.org(2006)) created by M. Nic, J. Jirat, B. Kosata; updates compiled by A. Jenkins. ISBN 0-9678550-9-8.
- Ivnitski, D., Abdel-Hamid, I., Atanasov, P., & Wilkins, E. (1999). Biosensors for detection of pathogenic bacteria. *Biosens. Bioelectron.* 14(1), 599-624.
- Jayasena, S.D. (1999). Aptamers: An emerging class of molecules that rival antibodies in diagnostics. *Clin. Chem.* 45(9), 1628-1650.
- Jenison, R.D., Gill, S.C., Pardi A., & Polisky, B. (1994). High-resolution molecular discrimination by RNA. *Science* 263(5152), 1425-1429.
- Jin, H., Leser, G. P., Zhang, J., & Lamb, R. A. (1997). Influenza virus hemagglutinin and neuraminidase cytoplasmic tails control particle shape. *EMBO J.* 16(6), 1236-1247.
- Jones, K.E., Patel, N.G., Levy, M.A., Storeygard, A., Balk, D., Gittleman, J.L., & Daszak, P. (2008). Global trends in emerging infectious diseases. *Nature* 451, 990-993.

- Karniadakis, G.M., Beskok, A., & Aluru, N. (2005). *Microflows and Nanoflows*. Springer. New York City.
- Lauerman, J. (2006). Indonesian bird flu cases may be sign of human spread. <http://www.bloomberg.com/apps/news?pid=newsarchive&sid=aWESsJvt6CFE&refer=asia>. Accessed July 19, 2014.
- Lee, C., & Saif, Y. M. (2009). Avian influenza virus. *Comp. Immunol. Microbiol. Infect.* 32(4), 301-310.
- Lee, S. H., Kim, S. W., Kang, J. Y., & Ahn, C. H. (2008). A polymer lab-on-a-chip for reverse transcription (RT)-PCR based point-of-care clinical diagnostics. *Lab Chip*. 8(12), 2121-2127.
- Lee, W. G., Kim, Y., Chung, B. G., Demirci, U., & Khademhosseini, A. (2010). Nano/Microfluidics for diagnosis of infectious diseases in developing countries. *Adv. Drug. Deliv.* 62(5), 449-457.
- Leland, D. S., & Ginocchio, C. C. (2007). Role of cell culture for virus detection in the age of technology. *Clin. Microbiol.* 20(1), 49-78.
- MacKay, W. G., van Loon, A. M., Niedrig, M., Meijer, A., Lina, B., & Niesters, H. G. M. (2008). Molecular detection and typing of influenza viruses: Are we ready for an influenza pandemic. *J. Clin. Virol.* 42(2), 194-197.
- Marandi, V. (2010). Assessment of a rapid immunochromatographic assay for the detection of avian influenza viruses. *Int. J. Vet. Res.* 4(3), 183-188.
- Medintz, I. L., Uyeda, H. T., Goldman, E. R., & Mattoussi, H. (2005). Quantum dot bioconjugates for imaging, labelling and sensing. *Nature* 4(6), 435-446.
- Phillips, K. S., & Cheng, Q. (2007). Recent advances in surface plasmon resonance based techniques for bioanalysis. *Anal. Bioanal. Chem.* 387(5), 1831-1840.
- National Instruments. (2012). *LabVIEW User Manual*. <http://www.ni.com/pdf/manuals/320999b.pdf>. Accessed July 27.
- Ohno, K., Tachikawa, K., & Manz, A. (2008). Microfluidics: Applications for analytical purposes in chemistry and biochemistry. *Electrophoresis* 29(22), 4443-4453.
- Pipper, J., Inoue, M., Ng, L. F., Neuzil, P., Zhang, Y., & Novak, L. (2007). Catching bird flu in a droplet. *Nature Med.* 75(10), 1259-1263.
- Sefah, K., Phillips, J.A., Xiong, X., Meng, L., Van Simaey, D., & Chen, H. (2009). Nucleic Acid aptamers for biosensors and bio-analytical applications. *Analyst* 134(1), 1765-1775.

- Seo, K. H., Brackett, R. E., Frank, J. F., & Hilliard, S. 1998. Immunomagnetic separation and flow cytometry for rapid detection of *Escherichia coli* 0157:H7. *J. Food Prot.* 61(7), 812-816.
- Stoltenburg, R, Reinemann, C, & Strehlitz, B. (2007). SELEX– a revolutionary method to generate high-affinity nucleic acid ligands. *Biomolec. Engr.* 24,381-403.
- Thomas, J.H., Kim, S.K., Hesketh, P.J., Halsall, H.B., & Heineman, W.R. (2004). Microbead based electrochemical immunoassay with interdigitated array microelectrodes. *Anal. Bioanal. Chem.* 328(2), 113-22.
- Thomas, J.K., & Noppenberger, J. (2007). Avian influenza: a review. *Health Syst. Pharm.* 64,149–65.
- Thorson, A., Petzold, M., Nguyen, T. K., & Ekdahl, K. (2006). Is exposure to sick or dead poultry associated with flulike illness: A population-based study from a rural area in Vietnam with outbreaks of highly pathogenic avian influenza. *Arch. Intern. Med.* 166(1), 119-123.
- Tuerk, C., & Gold, L. (1990). Systematic evolution of ligands by exponential enrichment: RNA ligands to bacteriophage T4 DNA polymerase. *Science* 249(4968), 505-510.
- Turner, A. P. F., Karube, I., & Wilson, G.S. (1987). *Biosensors Fundamentals and Applications*. Oxford University Press. Oxford, UK.
- Wong, S. S., & Yuen, K. Y. (2006). Avian influenza virus infections in humans. *Chest.* 129(1), 156-168.
- Wang, R., & Li, Y. (2013). Hydrogel based QCM aptasensor for detection of avian influenza Virus. *Biosens. Bioelectron.* 42(1), 148-155.
- WHO. (2012). Cumulative number of confirmed human cases for avian influenza A(H5N1) reported to WHO, 2003-2012. <http://www.who.int/influenza/humananimalinterface/CumulativeNumberH5N1cases.pdf>. Accessed May 18, 2014.
- Wikipedia. Microfluidics. <http://en.wikipedia.org/wiki/Microfluidics>. Accessed July 25, 2014.
- Wong, S. S., & Yuen, K. Y. (2006). Avian influenza virus infections in humans. *Chest.* 129(1), 156-168.
- Wu, G., & Yan, S. (2006). Prediction of possible mutations in H5N1 hemagglutinins of influenza A virus by means of logistic regression. *Comp. Clin. Pathol.* 15, 255-262.
- Zhang, B., Wang, R., Wang, Y., & Li, Y. (2013). A portable impedance biosensor for detection of multiple avian influenza viruses. *Sensors, 2013 IEEE.* 1-4.

Zhang, T., & Li, Y. (2013). A microelectrode flow cell system. China. Patent No.ZL201320023627.X.

Zhang, Y., Deng, Z., Yue, J., Tang, F., & Wei, Q. (2007). Using cadmium telluride quantum dots as a proton flux sensor and applying to detect H9 avian influenza virus.*Anal.Biochem.*364, 122-127.